

See discussions, stats, and author profiles for this publication at: <https://www.researchgate.net/publication/228439094>

# Fractal Structures of the Hydrogels Formed in Situ from Poly(N- isopropylacrylamide) Microgel Dispersions

ARTICLE in LANGMUIR · JULY 2012

Impact Factor: 4.46 · DOI: 10.1021/la3016386 · Source: PubMed

---

CITATIONS

7

---

READS

122

4 AUTHORS, INCLUDING:



Yongjun Zhang

Nankai University

89 PUBLICATIONS 1,792 CITATIONS

SEE PROFILE



X. X. Zhu

Université de Montréal

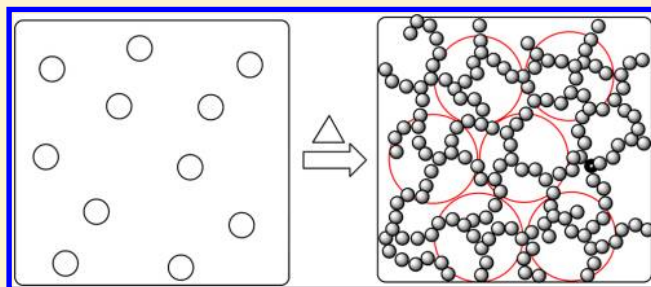
234 PUBLICATIONS 5,024 CITATIONS

SEE PROFILE

Fractal Structures of the Hydrogels Formed in Situ from Poly(*N*-isopropylacrylamide) Microgel DispersionsWang Liao,<sup>†</sup> Yongjun Zhang,<sup>\*,†</sup> Ying Guan,<sup>†</sup> and X. X. Zhu<sup>\*,‡</sup><sup>†</sup>State Key Laboratory of Medicinal Chemical Biology and Key Laboratory of Functional Polymer Materials, Institute of Polymer Chemistry, College of Chemistry, Nankai University, Tianjin 300071, China<sup>‡</sup>Department of Chemistry, Université de Montréal, C. P. 6128, Succursale Centre-ville, Montreal, QC, H3C 3J7, Canada

## S Supporting Information

**ABSTRACT:** Dispersions of poly(*N*-isopropylacrylamide) (PNIPAM) microgel thermally gel in the presence of inorganic salts. The in situ-formed hydrogels, with a network of soft particles, represent a new type of colloidal gels. Here, their fractal structures were determined by rheological measurements, using the models of both Shih et al. and Wu and Morbidelli. According to the definition of Shih et al., the colloidal PNIPAM gels fall into the strong-link regime. Yet the calculated fractal dimension of the floc backbone,  $\alpha$ , yielded unrealistic negative values, suggesting this model is inapplicable for the present system. The Wu–Morbidelli model gives physically sounder results. According to this model, the strengths of the inter- and intrafloc links are comparable, and the in situ-formed gels are in the transition regime. The fractal dimension,  $d_f$ , of the hydrogel decreases from  $\sim 2.5$  to  $\sim 1.8$  when the heating temperature increases from 34 to 40 °C. The  $d_f$  values suggest different aggregation mechanisms at different temperatures, that is, a reaction-limited one accompanied by rearrangement at low temperature, a typical reaction-limited one at the intermediate temperature, and a diffusion-limited one at high temperature. With increasing salt concentration, the  $d_f$  of the hydrogel decreases from  $\sim 2.1$  to  $\sim 1.7$ , suggesting the aggregation mechanism changes from reaction-limited to diffusion-limited. The effects of both temperature and salt concentration can be explained by the changes in the interactions among the microgel particles. The thermogellable PNIPAM microgel dispersions may serve as a model system for the study of heat-induced gelation of globular proteins.



## ■ INTRODUCTION

Microgels are small hydrogel particles with a size ranging from tens of nanometers to several micrometers.<sup>1,2</sup> Among them, the poly(*N*-isopropylacrylamide) (PNIPAM) microgel is perhaps the most extensively investigated. One reason lies in that monodisperse PNIPAM microgel is easy to synthesize by free-radical precipitation polymerization. More importantly, it undergoes a sharp volume phase transition when heated above a critical temperature. This material has found potential applications in a wide range of fields, especially in biomedical areas.<sup>3–5</sup>

Recently, we found that PNIPAM microgel dispersions thermally gel in the presence of inorganic salts.<sup>6</sup> The in situ-formed hydrogel can be developed as new injectable 3D cell scaffold. We have shown that this material is biocompatible and can support the growth and proliferation of various cells.<sup>6,7</sup> The new thermal gelling injectable scaffold is different from others in that microgel particles, instead of linear or branched polymers, are used as building blocks. Therefore, one may encapsulate growth factors or other bioactive molecules in the interior of the particles and release them in proper time to guide the differentiation of stem cells.<sup>8</sup> In addition, because of its reversibility, the new hydrogel can be used for the fabrication of multicellular spheroids.<sup>9</sup> To further exploit its application,

however, a deep understanding of the hydrogel structure is needed, as the performance of a 3D cell scaffold is strongly dependent on its internal structures.

The network structure of the new hydrogel is reminiscent of that of colloidal gels.<sup>10</sup> It is well-known that a lot of colloidal dispersions lose their colloidal stability and flocculate when the interactions among the colloidal particles become attractive. Under proper conditions, a continuous network of particles, which ultimately spans the whole system, will form.<sup>10–12</sup> The resulting solid-like materials are called colloidal gels, which have wide applications in the production of ceramics, food, medicine, controlled porous materials, and so on.<sup>13</sup> The new PNIPAM hydrogel is also a network of particles, and therefore can be regarded as a colloidal gel. Typical colloidal gels are composed of hard colloidal particles, of either an inorganic or a polymeric nature, for example, gold,<sup>14</sup> silica,<sup>15</sup> alumina,<sup>16</sup> and polymer latexes.<sup>13</sup> In contrast, the PNIPAM microgel particles are soft as they can deform and change their size in response to external forces.

Received: April 22, 2012

Revised: June 10, 2012

Published: July 6, 2012

In particular, the colloidal PNIPAM hydrogel is very similar to globular protein gels, which sometimes were treated as colloidal gels too.<sup>17,18</sup> Both PNIPAM microgel particles and globular proteins are spherical in shape, and both carry charges. Both systems gel by heating, and both in the presence of inorganic salt. The gelation of globular proteins was proposed to involve several steps.<sup>19</sup> First, the protein denatures under heating, exposing the hydrophobic or other reactive side chains, which are buried inside the core at ambient temperature. Next, the denatured protein molecules aggregate and finally form a 3D network. Similar steps can be found in the gelation of PNIPAM microgel dispersions. The first step is still the turning of the microgel particles from hydrophilic to hydrophobic as a result of the thermally induced phase transition. The shrunken particles then aggregate and finally form a 3D network.<sup>20</sup> Considering these similarities, the PNIPAM microgel dispersion may serve as a good model system for the study of the gelation of globular proteins. It is noteworthy that globular protein gels have received continuous attention because of their importance from both practical and scientific points of view; however, the mechanisms governing the gel network formation are not yet clear.<sup>17,18</sup>

Like other colloidal gels, especially globular protein gels, the colloidal PNIPAM gel also presents a highly disordered structure, as revealed by some preliminary SEM examinations.<sup>6,7</sup> For this kind of structures, fractal analysis is a suitable method for their description because they are self-similar in certain length scales.<sup>21</sup> In the framework of fractal theories, colloidal gels are considered to be a collection of fractal flocs closely packed throughout the system.<sup>17</sup> The dimensionless mass  $i$  of the fractal floc is assumed to scale with the radius of gyration  $R_{gi}$  by a power law:  $i = k_f(R_{gi}/R_p)^{d_f}$ , where the exponent  $d_f$  is the fractal dimension,  $R_p$  is the primary particle radius, and  $k_f$  is the fractal prefactor.<sup>12</sup> Various methods are available for the analysis of fractal structures of the aggregates or gels, including rheology, microscopy, and light scattering. As microscopic image analyses have difficulties in keeping the gel structure intact during sample preparation, and scattering techniques are usually only reliable for systems with a small particle volume fraction, rheological measurements are considered a better choice for the characterization of colloidal gels.<sup>17</sup>

In this work, the fractal structures of the colloidal PNIPAM gels were determined by rheological measurements, using two models deduced by Shih et al.<sup>16</sup> and Wu and Morbidelli,<sup>21</sup> respectively. The effects of temperature and salt concentration on the gel structure were studied. It was revealed that the aggregation mechanisms of the microgel dispersions are different under different gelling conditions and so are the structures of the resulting hydrogels. These results will direct our further efforts in the designing of new injectable cell scaffold with improved performance.

**Fractal Models.** In this article, two fractal models, that is, the model of Shih et al. and the Wu–Morbidelli model, were used, both of which are widely used in the literature. In 1990, Shih et al.<sup>16</sup> extended the earlier works of Brown and Ball,<sup>22</sup> Buscall et al.,<sup>23</sup> and Kantor and Webman,<sup>24</sup> and developed a fractal model by considering the structure of the gel network as a collection of flocs, which are fractal objects closely packed throughout the sample. They defined two regimes, that is, the strong-link regime where interfloc links are stronger than intrafloc links, and the weak-link regime where interfloc links are weaker than intrafloc links. In each regime, the elastic

constant of the gel, or storage modulus  $G'$ , and the limit of linearity,  $\gamma_0$ , have a scaling relationship with the particle volume fraction  $\phi$ .

In the strong-link regime:

$$G' \propto \phi^{(3+x)/(3-d_f)} \quad (1)$$

$$\gamma_0 \propto \phi^{-(1+x)/(3-d_f)} \quad (2)$$

Also, in the weak-link regime:

$$G' \propto \phi^{1/(3-d_f)} \quad (3)$$

$$\gamma_0 \propto \phi^{1/(3-d_f)} \quad (4)$$

where  $d_f$  is the fractal dimension of the flocs, and  $x$  is the fractal dimension of the floc backbone.

It is evident that the strong- and weak-link regimes described by the model of Shih et al. represent only two extreme situations, and the transition from one to the other must be continuous. Therefore, Wu and Morbidelli<sup>21</sup> further developed a scaling model in which an appropriate effective microscopic elastic constant,  $\alpha$ , was introduced to account for elastic contributions of both inter- and intrafloc links. It indicates the relative importance of these two contributions and allows for identification of which regime prevails in the system. On the basis of these considerations, scaling relationships between storage modulus  $G'$  or the limit of linearity  $\gamma_0$  and the particle volume fraction  $\phi$  were deduced:

$$G' \propto \phi^{\beta/(3-d_f)} \quad (5)$$

$$\gamma_0 \propto \phi^{(2-\beta)/(3-d_f)} \quad (6)$$

where  $\beta$  is an auxiliary parameter and defined as  $\beta = 1 + (2 + x)(1 - \alpha)$ .

## ■ EXPERIMENTAL SECTION

**Materials.** *N*-Isopropylacrylamide (NIPAM), *N,N'*-methylenebisacrylamide (BIS), potassium persulfate (KPS), and sodium dodecyl sulfate (SDS) were purchased from Aldrich or Acros. NIPAM was purified by recrystallization from a hexane/acetone mixture and dried in a vacuum.

**Microgel Synthesis.** PNIPAM microgel was prepared by free radical precipitation polymerization. First, 100 mL of reaction mixture containing 13.7 mM NIPAM, 3.0 mM BIS, and 0.4 mM SDS was prepared. It was bubbled with  $N_2$  and heated to 70 °C. After 1 h, 0.053 g of KPS (dissolved in 5 mL of water) was added to initiate the reaction. The reaction was allowed to proceed for 5 h. The resultant microgels were purified by dialysis (cutoff 12 000–14 000 Da) against water with frequent water change (at least twice daily) for 2 weeks.

**Dynamic Light Scattering.** Dynamic light scattering (DLS) characterization was performed on a Brookhaven 90Plus laser particle size analyzer at a scattering angle of 90°. The sample temperature was controlled with a built-in Peltier temperature controller. CONTIN algorithm was used for data analysis.

**Rheological Measurements.** Rheological tests were carried out on an AR2000ex rheometer (TA Instruments). Parallel aluminum plate geometry with a diameter of 60 mm was used. The temperature was controlled by a Peltier system on the bottom plate connected with a water bath. The sample gap was set to be 1.0 mm. Silicon oil was placed around the rim to prevent water evaporation during the experiments. Gels were formed by quick heating the samples from 15 °C to a predetermined temperature and then holding at the temperature for 1600 s. Then strain sweep measurements were carried out at the same temperature using a frequency of 1 rad/s.

## RESULTS AND DISCUSSION

### Thermal Gelation of PNIPAM Microgel Dispersions.

PNIPAM is a well-known thermosensitive polymer. It is hydrophilic and soluble in water at room temperature, but becomes relatively hydrophobic and precipitates from water when temperature rises above its LCST (lower critical solution temperature,  $\sim 31^\circ\text{C}$ ). Similarly, PNIPAM microgel particles are highly swollen in water at room temperature, but shrink when temperature rises above the VPTT (volume phase transition temperature, corresponding to LCST of linear polymer).<sup>1,2</sup> The thermosensitive behavior of the PNIPAM microgel used in this study is shown in Figure 1A. Its radius is

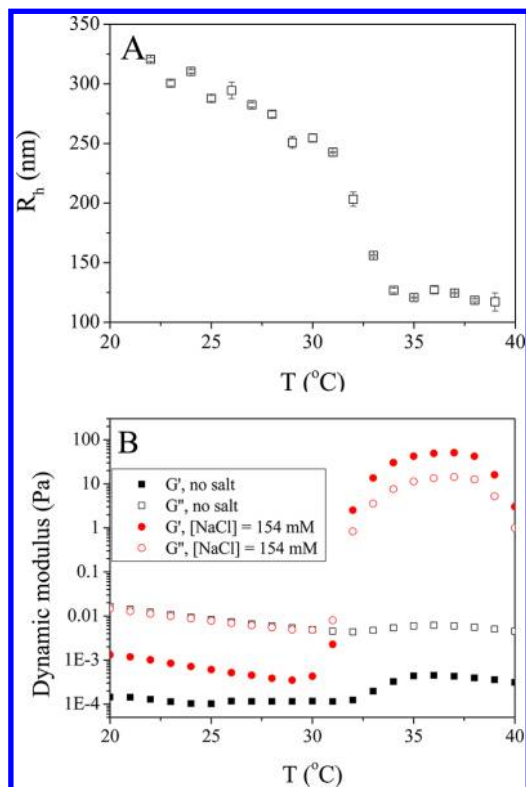


**Figure 1.** (A) Hydrodynamic radii ( $R_h$ ) of PNIPAM microgel as a function of temperature. (B) Evolution of storage modulus (solid symbols) and loss modulus (open symbols) of PNIPAM microgel dispersions with temperature increases measured at a frequency of 0.1 Hz and stress of 0.1 Pa.  $[\text{PNIPAM}] = 2.5 \text{ wt } \%$ .

$\sim 290 \text{ nm}$  at  $25^\circ\text{C}$ , but shrinks to  $\sim 145 \text{ nm}$  at  $37^\circ\text{C}$ . The VPTT of the sample, defined as the onset of the phase transition, is  $\sim 31^\circ\text{C}$ , which is in agreement with previous studies.<sup>20</sup>

Because of its thermosensitivity, under proper conditions, a concentrated PNIPAM microgel dispersion gels in situ upon heating. Figure 1B shows the evolution of the dynamic moduli,  $G'$  and  $G''$ , of a 2.5 wt % microgel dispersion containing 154 mM NaCl during a temperature ramp. At low temperature,  $G''$  dominates  $G'$ , indicating a liquid state. When temperature approaches the VPTT, both moduli increase sharply and crossover at  $\sim 31.8^\circ\text{C}$ . Beyond this point,  $G'$  always dominates  $G''$ , indicating the formation of a 3D network. In contrast, another microgel dispersion of the same concentration but containing no NaCl does not gel, indicating adding inorganic salt is critical for the thermal gelation of PNIPAM microgel dispersions (Figure 1B). As we pointed out previously,<sup>6,7</sup> the

colloidal stability of the microgel dispersions containing no salt is attributed to the negatively charged groups incorporated on the surface of the microgel particles during polymerization. The added salt screens the electrostatic repulsion among the microgel particles (it also depresses the VPTT),<sup>1</sup> allowing them to aggregate and form a 3D network upon heating.

**Determination of Storage Modulus  $G'$  and Critical Strain  $\gamma_c$ .** Thermal gelation of the salt-containing microgel dispersions can also be achieved by isothermal heating, that is, quick heating of the dispersions to a predetermined temperature above the critical gelation temperature and then holding at this temperature.<sup>25,26</sup> In the remaining part of the work, in situ gelation of the microgel dispersions was all achieved by isothermal heating. Changes in the dynamic moduli,  $G'$  and  $G''$ , of the dispersions with time were monitored. Figure 2 shows a

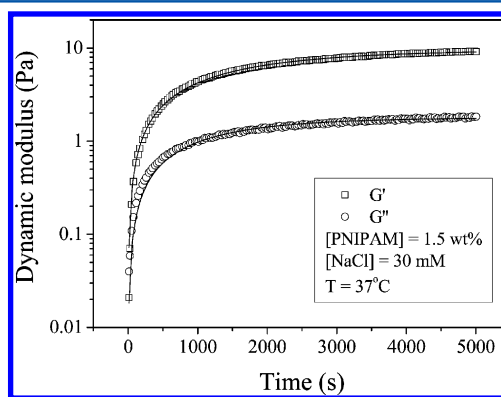


**Figure 2.** Evolution of dynamic modulus of a 1.5 wt % PNIPAM microgel dispersion with time measured at a frequency of 1 rad/s and strain of 4% when isothermally heated at  $37^\circ\text{C}$ .  $[\text{NaCl}] = 30 \text{ mM}$ . The lines were obtained from curve fitting, using first-order function,  $G(t) = G_\infty(1 - e^{-bt})$ .

typical example. One can see that both  $G'$  and  $G''$  increase sharply with time during this heating process and  $G'$  overpasses  $G''$  quickly. The result indicates that the dispersion thermally gels very quickly, which is in agreement with our previous observations.<sup>20</sup> After the initial quick increase, the increase rate of  $G'$  and  $G''$  slows gradually. Both moduli seem to approach a plateau upon extended heating. The evolution of  $G$  ( $G'$  or  $G''$ ) with heating time can be well-fitted using a simple first-order function,  $G(t) = G_\infty(1 - e^{-bt})$ , as shown in Figure 2. Similar first-order reaction kinetics has been widely observed in the thermal gelation of globular proteins and other colloidal gels.<sup>17,18,27</sup>

The fractal models of Shih et al. and Wu and Morbidelli directly relate the microscopic structural parameters of a colloidal gel to its macroscopic elastic properties. To calculate  $d_f$  of the colloidal PNIPAM hydrogel using these models, one should first determine the elastic modulus,  $G'$ , and the limit of linearity,  $\gamma_0$ , of the gel. As for  $G'$ , as shown in Figure 2, it continues changing with time. No real plateau was reached even after an extended heating. In this case, one may predict  $G'$  at an infinite time,  $G'_\infty$ , using the first-order function,  $G(t) = G_\infty(1 - e^{-bt})$ , which fits the  $G'$ -time curves very well as shown in Figure 2. Another choice is the direct adoption of the  $G'$  value at an appropriate heating time. This approach has previously used by Ikeda et al. when studying the fractal structure of a protein gel.<sup>17</sup> We also adopted this approach considering that two values, that is, the elastic modulus,  $G'$ , and the limit of



linearity,  $\gamma_0$ , are needed to determine  $d_f$ . Although  $G'_\infty$  can be predicted by curve fitting,  $\gamma_0$  can only be measured at a finite heating time. Therefore, it will be more appropriate to use the values of  $G'$  and  $\gamma_0$  measured at the same time.

In this work, we choose a heating time of 1600 s. From Figure 2, an inflection point was observed at a heating time of 500–700 s. From then on, the  $G'$  increment slows gradually, indicating the change in the gel structure is not as evident as before. After being heated for 1600 s, which is about 3 times the inflection time, the  $G'$  increment slows significantly, making it a good point for the determination of fractal structures. The microgel dispersions were isothermally heated for 1600 s and then subjected to a strain sweep.  $G'$  value at the plateau area was determined as  $G'$  of the in situ-formed hydrogel, as shown in Figure 3.

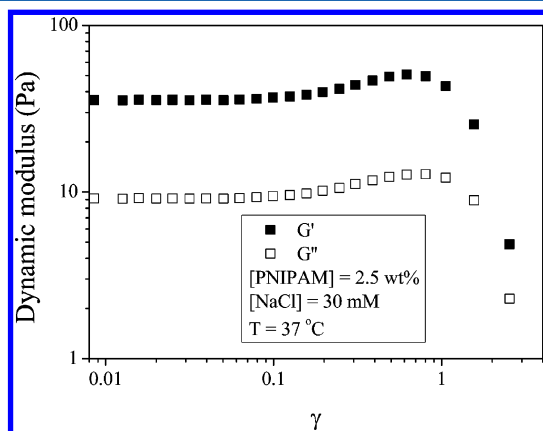


**Figure 3.** Storage and loss moduli ( $G'$  and  $G''$ ) of an in situ-formed gel as a function of strain amplitude. [PNIPAM] = 2.5 wt %, [NaCl] = 30 mM. The gel was obtained by isothermal heating at 37 °C for 1600 s.

The limit of linearity,  $\gamma_0$ , was also determined from the strain sweep experiment (Figure 3). For thermally gelled protein hydrogels,  $G'$  remains almost constant and then suddenly decreases as the strain increases.<sup>18</sup> Similar behaviors were observed from the colloidal gel of Dispal boehmite alumina.<sup>16</sup> The sudden decrease in  $G'$  indicates the breakage of bonds within the gel network, resulting in a transition from a linear to a nonlinear behavior. For these systems, the strain amplitude at which  $G'$  just begins to decrease by 5% from its maximum value was taken as a measure of the limit of linearity,  $\gamma_0$ , of the gel.<sup>16,18,27</sup> For the colloidal PNIPAM gel studied here, however, linear response was only observed when the applied strain,  $\gamma$ , is less than 0.1 (Figure 3). Further increase in strain amplitude results in a slight increase in both  $G'$  and  $G''$ . Finally, when  $\gamma$  approaches  $\sim 0.9$ , both moduli drop precipitously. Similar strain hardening has been observed from various hydrogels,<sup>28,29</sup> including colloidal hydrogels and protein gels.<sup>30,31</sup> The origin of the strain hardening in these systems remains obscure. Gisler et al. attributed the strain hardening in colloidal gels to the contorted backbone of the gel, which can be lengthened under a large shear strain and thus increase the rigidity of the gel.<sup>30</sup> Considering the strain hardening observed here is relatively weak, we still take the strain amplitude at which  $G'$  just begins to decrease by 5% from its maximum value as the critical strain of the gel.<sup>16,18,27</sup> We take the term “critical strain” instead of “limit of linearity” because the behavior of the gel is no longer linear when strain hardening occurs. Despite this, the critical strain is still a good measure of the strength of the weakest

bonds in the gel, just like the limit of linearity in the mode of Shih et al.<sup>16</sup> It is noteworthy that a weak strain hardening can also be detected from the colloidal gel in Shih et al.’s work, which was used to test their model.<sup>16</sup>

**Fractal Structure of the Colloidal PNIPAM Gels.** Using the above methods, the storage modulus  $G'$  and critical strain  $\gamma_c$  of the in situ-formed gels can be determined. They can be scaled with microgel concentration [PNIPAM]. Fractal structure of the gel can be further determined using the model of Shih et al. or the Wu–Morbidelli model.

One important factor influencing the gel structure is the temperature at which the dispersions gelled. To study this factor, a series of microgel dispersions, with a constant NaCl concentration of 30 mM, were gelled by isothermal heating at various temperatures. The storage modulus  $G'$  and critical strain  $\gamma_c$  of the in situ-formed gels were measured and plotted as a function of [PNIPAM] as shown in Figure 4A and B,

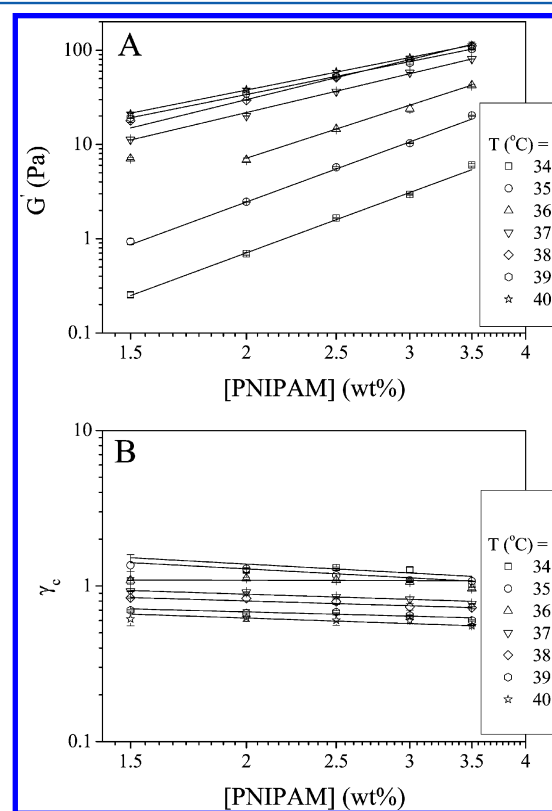


**Figure 4.** Double-logarithmic plots of the storage modulus  $G'$  (A) and critical strain  $\gamma_c$  (B) of the hydrogels gelled at various temperatures as a function of microgel concentration. [NaCl] = 30 mM.

respectively. It is noteworthy that the concentration range studied here is relatively narrow because of the experimental difficulties. Similar concentration ranges were used in the literatures, possibly due to the same reason.<sup>16,17</sup>

As expected, both  $G'$  and  $\gamma_c$  exhibit a power-law behavior or a scaling relationship with microgel concentration that can be fitted to the form:  $G' \approx C^m$  or  $\gamma_c \approx C^n$ , where  $m$  and  $n$  are the power-law exponents.  $n$  values are positive for all gels and vary from  $\sim 2.0$  to  $3.6$ . Previously,  $n$  values varying from  $2.0$  to  $11$  were reported for protein gels.<sup>18</sup> In contrast,  $m$  values are all negative, varying from  $-0.01$  to  $-0.33$ .

According to Shih et al.’s definition, the in situ-formed gel can be regarded to fall into the strong-link regime, because  $G'$

increases, but  $\gamma_c$  decreases with increasing microgel concentration.<sup>16</sup> Therefore, the fractal dimension  $d_f$  of the gel was determined using eqs 1 and 2, which varies from 1.85 to 2.4 (Figure 1SA). The calculations simultaneously give the fractal dimension of the floc backbone,  $x$ , which varies between  $-0.77$  and  $-1.0$  (Figure 1SB). It was pointed out that reasonable values for  $x$  usually lie in the range of  $1-1.3$ .<sup>21</sup> Therefore, the  $x$  values derived from the model of Shih et al. are unrealistic, suggesting the inapplicability of the model for the present system.<sup>18,21</sup> In fact,  $\gamma_c$  of the in situ formed gel only slightly decreases with increasing microgel concentration. The determined values of the power-law exponent  $m$  are all very close to 0. In contrast, for strong-link colloidal gels such as the Catapal and Dispal gels studied by Shih et al., the power-law exponent  $m$  was determined to be  $-2.1$  and  $-2.3$ , respectively.<sup>16</sup> Correspondingly,  $\gamma_c$  of these gels is highly dependent on the colloidal concentrations.

Because the model of Shih et al. is inapplicable for the present system, we turned to the Wu–Morbidelli model, which attributes the effective elastic property of a colloidal gel to the mutual elastic contributions of both inter- and intrafloc links.<sup>21</sup> Using eqs 5 and 6, one can estimate the fractal dimension,  $d_f$ , and an auxiliary parameter,  $\beta$ . Assuming the backbone fractal dimension  $x$  lies in the range  $[1, 1.3]$ , one can further determine the value of  $\alpha$ , which reflects the relative contributions of the inter- and intrafloc links. Using this approach,  $d_f$  values of the gels formed at various temperatures were determined and plotted in Figure 5A. As compared to the results shown in Figure 1SA,  $d_f$  values derived from the two models are comparable, but the Wu–Morbidelli model is physically more consistent. Figure 5B shows the corresponding

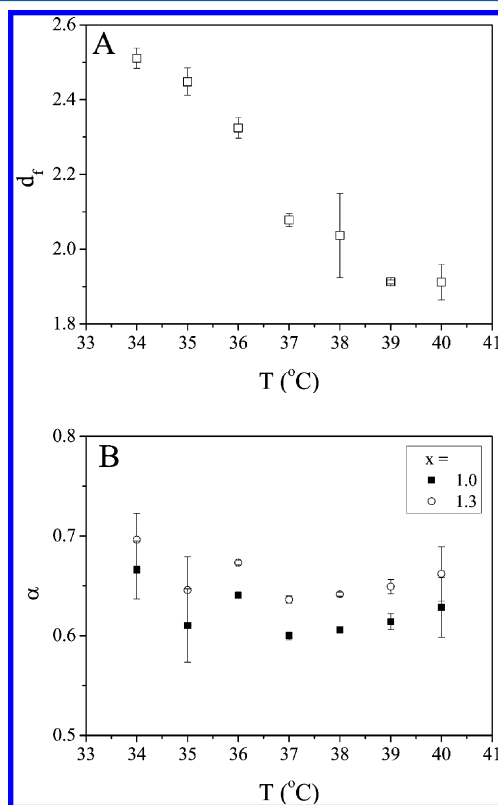


**Figure 5.** (A) Fractal dimension,  $d_f$ , and (B) the parameter,  $\alpha$ , of the in situ-formed gels gelled at various temperatures. The results were calculated from the data in Figure 4 using the Wu–Morbidelli model.

values of  $\alpha$ . One can see it varies between 0.6 and 0.7, clearly indicating the in situ-formed gels fall into the transition regime.

Another important factor influencing the gel structure is the concentration of NaCl added to the dispersions. To study this factor, a series of microgel dispersions, with NaCl concentration varying from 30 to 270 mM, were gelled by isothermal heating at 37 °C. The storage modulus  $G'$  and critical strain  $\gamma_c$  of the in situ-formed gels were plotted in Figure 6A and B as a function

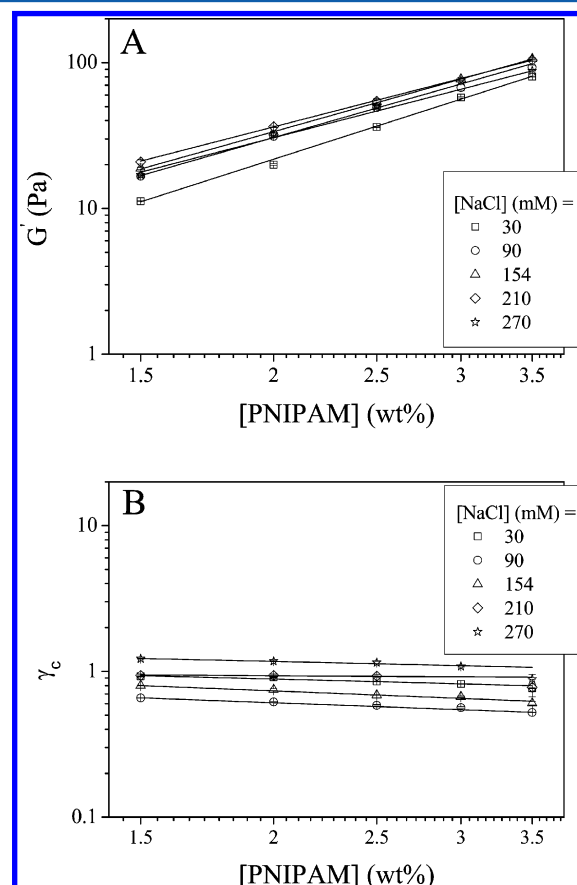


**Figure 6.** Double-logarithmic plots of the storage modulus  $G'$  (A) and critical strain  $\gamma_c$  (B) of the hydrogels formed in situ as a function of microgel concentration. The gels formed at 37 °C in the presence of various concentration of NaCl.

of [PNIPAM]. Again, a good scaling relationship between rheological properties ( $G'$  and  $\gamma_c$ ) and microgel concentration was found. Fractal dimensions of the gels were calculated using the model of Shih et al. (Figure 2S) and the Wu–Morbidelli model (Figure 7), respectively. Again, the unrealistic negative values of the backbone fractal dimension  $x$  derived from the model of Shih et al. suggest the inapplicability of this model (Figure 2SB). The Wu–Morbidelli model is physically sounder. The value of  $\alpha$  derived from this model varies between 0.54 and 0.64, indicating the in situ-formed gels fall into the transition regime.

**Aggregation Mechanisms.** From the above analysis, we obtained two parameters, that is,  $d_f$  and  $\alpha$ , both of which contain important information about the gel structure. The parameter  $\alpha$  is a measure of the relative importance of the contributions of the inter- and intrafloc links. The values of  $\alpha$  obtained here (from 0.54 to 0.70) indicate the contributions from inter- and intrafloc links are comparable.<sup>21</sup> The results are reasonable, considering that both inter- and intrafloc links are

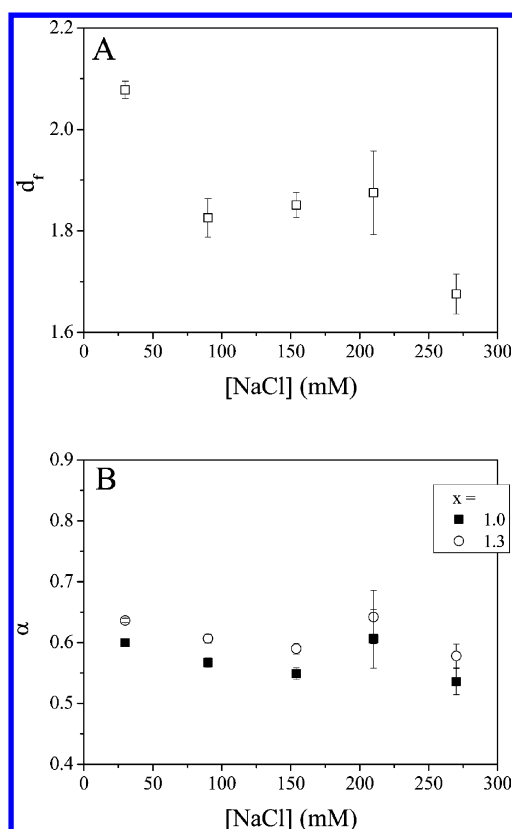


**Figure 7.** (A) Fractal dimension,  $d_f$ , and (B) the parameter,  $\alpha$ , of the gels formed in situ in the presence of various concentrations of NaCl. The results were calculated from the data in Figure 6 using the Wu–Morbidelli model.

formed by hydrophobic interaction; therefore, there is no big difference in their strengths. In addition, the value of parameter  $\alpha$  does not significantly change with the heating temperature (Figure 5B) or NaCl concentration (Figure 7B). Interestingly, the parameter  $\alpha$  obtained here is close to that of many globular protein gels. By reproducing other authors' experimental data,<sup>17,32</sup> Wu and Morbidelli obtained an  $\alpha$  value of 0.76 for heat-induced  $\beta$ -lactoglobulin protein gel and  $\alpha$  values ranging from 0.5 to 0.7 for heat-induced whey protein isolate gels.<sup>21</sup> However, the  $\alpha$  values for heat-induced egg white gel at various pH's are relatively small (from 0.05 to 0.50).<sup>18</sup>

More importantly, the fractal dimension  $d_f$  indicates the stacking density of the particles in the fractal flocs. As shown in Figure 5A,  $d_f$  of the in situ-formed hydrogel decreases gradually from 2.5 to 1.9 with increasing heating temperature from 34 to 40 °C, indicating denser fractal flocs form at a relatively low temperature and looser fractal flocs form at a relatively high temperature. More importantly, the value of  $d_f$  reflects the aggregation mechanism of the colloidal gel. It has long been revealed that colloidal aggregates grown in the reaction-limited and diffusion-limited aggregation regimes are characterized by fractal dimensions of 2.0–2.2 and 1.7–1.8, respectively, according to both computer simulations and experimental results.<sup>12,14,17,18,33,34</sup> In addition, in some cases, restructuring may take place, resulting in an increase in  $d_f$  of the final structure.<sup>33,35</sup> Therefore, the aggregation mechanism of the in situ-formed hydrogels can be conjectured from their fractal structures. When gelled in the temperature range of 34–36 °C,  $d_f$  was determined to be 2.3–2.5, indicating a reaction-limited aggregation accompanied by significant restructuring.<sup>35</sup> When

gelled in the temperature range of 37–38 °C, the gelation is achieved mainly via reaction-limited aggregation; therefore,  $d_f$  falls in the range of 2.0–2.1. Further increasing the heating temperature to 39 and 40 °C results in diffusion-limited aggregation. Therefore,  $d_f$  of the resulting hydrogel further reduces to close to 1.8.

The possible mechanism derived from  $d_f$  values is reasonable considering the change in the interaction among the microgel particles. It is well-known that PNIPAM polymer becomes hydrophobic at a temperature higher than its LCST, and it becomes more hydrophobic with increasing temperature. The heating temperatures studied here are all above its LCST. When heated at relatively low temperatures (34–36 °C, slightly higher than LCST), the interaction among the particles is not strong; therefore, the aggregation is slow. Also, the relatively weak interaction makes it possible for the rearrangement of the particles to occur. At intermediate temperatures (37–38 °C), the interaction becomes stronger. Although the aggregation is still slow, rearrangement is now forbidden; therefore, the system displays a typical reaction-limited behavior. With further increasing temperature, the interaction is so strong that the particles aggregate at a fast speed, leading to a diffusion-limited aggregation. Previously, Routh et al.<sup>36</sup> studied the salt-induced aggregation of copolymer microgel of NIPAM and acrylic acid in diluted solutions. They determined the fractal dimension of the aggregates by static light scattering and found it drops from 2.0 at 34 °C to 1.75 at 40 °C, indicating a similar transition from reaction-limited aggregation to diffusion-limited aggregation.

Figure 7A shows the effect of NaCl concentration on  $d_f$  of the hydrogels formed in situ at 37 °C. When [NaCl] is only 30 mM,  $d_f$  of the hydrogel was determined to be ~2.1, suggesting a reaction-limited aggregation. The heating temperature is already sufficiently higher than the VPTT of the microgel, but the negatively charged groups on the microgel surface are not effectively screened by NaCl. Therefore, the particle aggregation is not fast, resulting in a reaction-limited aggregation. However, hydrogels formed at higher [NaCl] display a  $d_f \approx 1.8$ , indicating they form via a diffusion-limited aggregation. In these cases, the negative charges of the microgel particles were screened more effectively by NaCl, resulting in a fast aggregation of the particles and diffusion-limited aggregation. In addition, higher [NaCl] also decreases the VPTT of PNIPAM microgels because the aqueous solution becomes an increasingly poorer solvent for PNIPAM at higher [NaCl].<sup>20,37–39</sup> Therefore, the microgel particles become more hydrophobic and attractions among them are stronger, which is the second reason for the fast aggregation of the particles. It is noteworthy that the effect of salt concentration on the fractal dimension of the individual flocs was not studied yet because of experimental difficulties. Previously, Rasmusson et al.<sup>39</sup> determined the fractal dimension of the individual flocs at temperatures close to the critical flocculation temperature by dynamic light scattering. A value of 2.0 was obtained, indicating a reaction-limited aggregation. They expected that  $d_f$  will decrease with increasing NaCl concentration. The results shown in Figure 7A can be regarded as a proof of their expectation.

The effect of salt concentration on the fractal structure of PNIPAM hydrogel is quite similar to that of globular protein gels. Salt concentration is also one of the major factors influencing the microscopic network structure of globular protein gels. Previously, Ikeda et al.<sup>17</sup> found the fractal

dimension of the heat-induced whey protein isolate (WPI) gels is  $\sim 2.2$  at 25 mM NaCl. Further addition of NaCl (50–1000 mM) decreased the value to  $\sim 1.8$ . The two systems behave similarly because the effect of salt is similar, that is, altering the balance between attractive and repulsive forces, mainly through electrostatic shielding effects.

## CONCLUSIONS

The fractal structures of the colloidal PNIPAM gels were determined by rheological measurements. Two fractal models, that is, the model of Shih et al. and the Wu–Morbidelli model, were used to calculate the fractal dimension of the gels from their rheological properties. The colloidal PNIPAM gels fall into the strong-link regime according to the definition of Shih et al., but it yields negative values for the fractal dimension of the floc backbone, making it inapplicable in this system. According to the Wu–Morbidelli model, the strengths of the inter- and intrafloc links are comparable, and the in situ-formed gels are in the transition regime. The effects of temperature and salt concentration were studied. As the heating temperature increases from 34 to 40 °C, the  $d_f$  of the hydrogel decreases from  $\sim 2.5$  to  $\sim 1.8$ , reflecting the transition of the aggregation mechanism from a reaction-limited one accompanied by rearrangement to typical reaction-limited, and finally diffusion-limited. With increasing salt concentration, the  $d_f$  of the hydrogel decreases from  $\sim 2.1$  to  $\sim 1.7$ . The aggregation mechanism changes from reaction-limited to diffusion-limited. The effects of temperature and salt concentration on the aggregation mechanism can be explained by the changes in the interactions among the microgel particles.

## ASSOCIATED CONTENT

### Supporting Information

Fractal dimension,  $d_p$ , and the fractal dimension of the floc backbone,  $\alpha$ , of the in situ-formed gels calculated using the model of Shih et al. This material is available free of charge via the Internet at <http://pubs.acs.org>.

## AUTHOR INFORMATION

### Corresponding Author

\*E-mail: [yongjunzhang@nankai.edu.cn](mailto:yongjunzhang@nankai.edu.cn) (Y.Z.); [julian.zhu@umontreal.ca](mailto:julian.zhu@umontreal.ca) (X.X.Z.).

### Notes

The authors declare no competing financial interest.

## ACKNOWLEDGMENTS

We are thankful for financial support for this work from the National Natural Science Foundation of China (Grants Nos. 20974049, 20974050, and 21174070), the Tianjin Committee of Science and Technology (10JCYBJC02000), the Program for New Century Excellent Talents in University (NCET-11-0264), and the Ministry of Science and Technology of China (Grant No.: 2007DFA50760).

## REFERENCES

- (1) Saunders, B. R.; Vincent, B. Microgel particles as model colloids: theory, properties and applications. *Adv. Colloid Interface Sci.* **1999**, *80*, 1–25.
- (2) Pelton, R. Temperature-sensitive aqueous microgels. *Adv. Colloid Interface Sci.* **2000**, *85*, 1–33.
- (3) Saunders, B. R.; Laajam, N.; Daly, E.; Teow, S.; Hu, X. H.; Stepto, R. Microgels: From responsive polymer colloids to biomaterials. *Adv. Colloid Interface Sci.* **2009**, *147–48*, 251–262.
- (4) Lyon, L. A.; Meng, Z. Y.; Singh, N.; Sorrell, C. D.; John, A. S. Thermoresponsive microgel-based materials. *Chem. Soc. Rev.* **2009**, *38*, 865–874.
- (5) Guan, Y.; Zhang, Y. PNIPAM microgels for biomedical applications: from dispersed particles to 3D assemblies. *Soft Matter* **2011**, *7*, 6375–6384.
- (6) Gan, T.; Zhang, Y.; Guan, Y. In situ gelation of P(NIPAM-HEMA) microgel dispersion and its applications as injectable 3D cell scaffold. *Biomacromolecules* **2009**, *10*, 1410–1415.
- (7) Gan, T. T.; Guan, Y.; Zhang, Y. J. Thermogelable PNIPAM microgel dispersion as 3D cell scaffold: effect of syneresis. *J. Mater. Chem.* **2010**, *20*, 5937–5944.
- (8) Jaklenec, A.; Wan, E.; Murray, M. E.; Mathiowitz, E. Novel scaffolds fabricated from protein-loaded microspheres for tissue engineering. *Biomaterials* **2008**, *29*, 185–192.
- (9) Wang, D.; Cheng, D.; Guan, Y.; Zhang, Y. Thermoreversible hydrogel for in situ generation and release of HepG2 spheroids. *Biomacromolecules* **2011**, *12*, 578–584.
- (10) Trappe, V.; Sandkuhler, P. Colloidal gels - low-density disordered solid-like states. *Curr. Opin. Colloid Interface Sci.* **2004**, *8*, 494–500.
- (11) Lu, P. J.; Zaccarelli, E.; Ciulla, F.; Schofield, A. B.; Sciortino, F.; Weitz, D. A. Gelation of particles with short-range attraction. *Nature* **2008**, *453*, 499–U4.
- (12) Sandkuhler, P.; Lattuada, M.; Wu, H.; Sefcik, J.; Morbidelli, M. Further insights into the universality of colloidal aggregation. *Adv. Colloid Interface Sci.* **2005**, *113*, 65–83.
- (13) Wu, H.; Tsoutsoura, A.; Lattuada, M.; Zaccone, A.; Morbidelli, M. Effect of temperature on high shear-induced gelation of charge-stabilized colloids without adding electrolytes. *Langmuir* **2010**, *26*, 2761–2768.
- (14) Lin, M. Y.; Lindsay, H. M.; Weitz, D. A.; Ball, R. C.; Klein, R.; Meakin, P. Universality in colloid aggregation. *Nature* **1989**, *339*, 360–362.
- (15) Kegel, W. K.; Lekkerkerker, H. N. W. Colloidal gels: Clay goes patchy. *Nat. Mater.* **2011**, *10*, 5–6.
- (16) Shih, W.; Shih, W. Y.; Kim, S.; Liu, J.; Aksay, I. A. Scaling behavior of the elastic properties of colloidal gels. *Phys. Rev. A* **1990**, *42*, 4772.
- (17) Ikeda, S.; Foegeding, E. A.; Hagiwara, T. Rheological study on the fractal nature of the protein gel structure. *Langmuir* **1999**, *15*, 8584–8589.
- (18) Eleya, M. M. O.; Ko, S.; Gunasekaran, S. Scaling and fractal analysis of viscoelastic properties of heat-induced protein gels. *Food Hydrocolloids* **2004**, *18*, 315–323.
- (19) Gosal, W. S.; Ross-Murphy, S. B. Globular protein gelation. *Curr. Opin. Colloid Interface Sci.* **2000**, *5*, 188–194.
- (20) Liao, W.; Zhang, Y.; Guan, Y.; Zhu, X. X. Gelation kinetics of thermosensitive PNIPAM microgel dispersions. *Macromol. Chem. Phys.* **2011**, *212*, 2052–2060.
- (21) Wu, H.; Morbidelli, M. A model relating structure of colloidal gels to their elastic properties. *Langmuir* **2001**, *17*, 1030–1036.
- (22) Brown, W. D.; Ball, R. C. Computer simulation of chemically limited aggregation. *J. Phys. A: Math. Gen.* **1985**, *18*, L517.
- (23) Buscall, R.; Mills, P. D. A.; Goodwin, J. W.; Lawson, D. W. Scaling behaviour of the rheology of aggregate networks formed from colloidal particles. *J. Chem. Soc., Faraday Trans. 1* **1988**, *84*, 4249–4260.
- (24) Kantor, Y.; Webman, I. Elastic properties of random percolating systems. *Phys. Rev. Lett.* **1984**, *52*, 1891–1894.
- (25) Tobitani, A.; Ross-Murphy, S. B. Heat-induced gelation of globular proteins. 1. Model for the effects of time and temperature on the gelation time of BSA gels. *Macromolecules* **1997**, *30*, 4845–4854.
- (26) Kavanagh, G. M.; Clark, A. H.; Ross-Murphy, S. B. Heat-induced gelation of globular proteins: 4. Gelation kinetics of low pH beta-lactoglobulin gels. *Langmuir* **2000**, *16*, 9584–9594.
- (27) Rueb, C. J.; Zukoski, C. F. Viscoelastic properties of colloidal gels. *J. Rheol.* **1997**, *41*, 197–218.



- (28) He, J.; Zhang, A.; Zhang, Y.; Guan, Y. Novel redox hydrogel by in situ gelation of chitosan as a result of template oxidative polymerization of hydroquinone. *Macromolecules* **2011**, *44*, 2245–2252.
- (29) Maiti, M.; Bhowmick, A. K. Dynamic viscoelastic properties of fluoroelastomer/clay nanocomposites. *Polym. Eng. Sci.* **2007**, *47*, 1777–1787.
- (30) Gisler, T.; Ball, R. C.; Weitz, D. A. Strain hardening of fractal colloidal gels. *Phys. Rev. Lett.* **1999**, *82*, 1064–1067.
- (31) Pouzot, M.; Nicolai, T.; Benyahia, L.; Durand, D. Strain hardening and fracture of heat-set fractal globular protein gels. *J. Colloid Interface Sci.* **2006**, *293*, 376–383.
- (32) Hagiwara, T.; Kumagai, H.; Matsunaga, T. Fractal analysis of the elasticity of BSA and  $\beta$ -lactoglobulin gels. *J. Agric. Food Chem.* **1997**, *45*, 3807–3812.
- (33) Meakin, P.; Jullien, R. The effects of restructuring on the geometry of clusters formed by diffusion-limited, ballistic, and reaction-limited cluster–cluster aggregation. *J. Chem. Phys.* **1988**, *89*, 246–250.
- (34) Schaefer, D. W.; Martin, J. E.; Wiltzius, P.; Cannell, D. S. Fractal geometry of colloidal aggregates. *Phys. Rev. Lett.* **1984**, *52*, 2371–2374.
- (35) Echeverria, C.; Lopez, D.; Mijangos, C. UCST responsive microgels of poly(acrylamide-acrylic acid) copolymers: Structure and viscoelastic properties. *Macromolecules* **2009**, *42*, 9118–9123.
- (36) Routh, A. F.; Vincent, B. Salt-induced homoaggregation of poly(*N*-isopropylacrylamide) microgels. *Langmuir* **2002**, *18*, 5366–5369.
- (37) Park, T. G.; Hoffman, A. S. Sodium chloride-induced phase transition in nonionic poly(*N*-isopropylacrylamide) gel. *Macromolecules* **1993**, *26*, 5045–5048.
- (38) Daly, E.; Saunders, B. R. A study of the effect of electrolyte on the swelling and stability of poly(*N*-isopropylacrylamide) microgel dispersions. *Langmuir* **2000**, *16*, 5546–5552.
- (39) Rasmusson, M.; Routh, A.; Vincent, B. Flocculation of microgel particles with sodium chloride and sodium polystyrene sulfonate as a function of temperature. *Langmuir* **2004**, *20*, 3536–3542.